

Amorphous Thin Film Growth: Modeling and Pattern Formation

Stefan J. Linz, Martin Raible, and Peter Hänggi

Theoretische Physik I, Institut für Physik, Universität Augsburg,
86135 Augsburg, Germany

Abstract. We report on recent progress on the theoretical description of amorphous thin film growth generated by physical vapor deposition. Specifically, we motivate a minimal model for the spatio-temporal evolution of the surface morphology that incorporates the dominant relaxation mechanisms of the deposition and agglomeration process. The characteristic statistical measures of the surface morphology such as the correlation length and the surface roughness calculated from this model show very good agreement with available experimental data and, therefore, support the validity of the modeling approach.

The formation and spatio-temporal evolution of interfaces by deposition processes are ubiquitous phenomena in nature [1,2]. Such a surface growth can be observed on macroscopic scales, e.g. during the aggregation of snow flakes or the heap formation as consequence of the downpour of granular material, as well as on the technologically more important microscopic scales in form of atom deposition as, e.g., in molecular beam epitaxy or physical vapor deposition. Unraveling nature's hidden rules of building up such agglomerations of particles and their corresponding surface structure constitutes one of the central challenges of modern condensed matter physics in the last three decades. An overall theoretical understanding of the surface growth kinetics during atom deposition processes is still at an early stage; technologically desired theoretical tools to aid the systematic control and optimization of the surface structure are still far beyond our present knowledge. An important theoretical step in this direction might be the concept of field equations [1-3] that should be able to model the nanoscale evolution of the surface structure of atom deposition processes if the dominant system-specific relaxation mechanisms of the deposited particles are appropriately taken into account.

In this contribution, we specifically focus on the growth of solid amorphous films generated by physical vapor deposition that is important e.g. in the context of coating and the manufacturing of thin glassy ZrAlCu films and has recently attracted interest [4-7] in materials science. We review and partly extend some major results obtained in recent works [7-9] on the development and detailed analysis of a minimal model in form of a stochastic field equation that (i) appropriately describes the spatio-temporal evolution of such amorphous surface growth processes and (ii) stands the test of a quantitative comparison with available experimental data [4-7]. From the

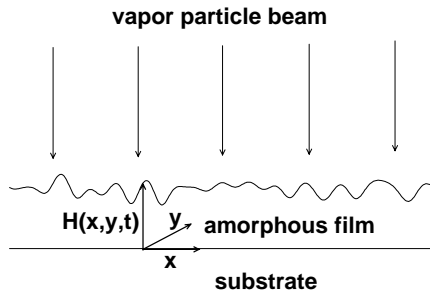


Fig. 1. Sketch of a vapor deposition experiment for amorphous thin film growth

theoretical point of view, amorphous film growth constitutes a particularly attractive testing ground for a *quantitative* comparison of experimental data and theoretical approaches since (i) there are not any long range ordering phenomena (as in epitaxial growth processes) to be expected, (ii) the effect of terrace formation and, therefore, the Ehrlich-Schwoebel effect being significant for epitaxial growth processes are absent, and (iii) the growing film should be spatially isotropic.

Our contribution is organized as follows. In section 1, we briefly review the basics of the considered experimental system and the analyzing tools for the surface morphology. In section 2, we motivate the functional form of the appropriate model equation and, in section 3, relate the entering terms to the underlying physical relaxation mechanisms of the deposited particles. Section 4 deals with the comparison of numerical simulations of the growth equation and experimental data being available up to a film height of 480nm; predictions for the subsequent evolution of the film up to 2000nm are given in section 5. For further results, we refer to the references [7–10].

1 Basics

The generic setup of a film growth process, cf. also Fig. 1, consists of an initially almost flat substrate and a vapor particle beam that is determined by the deposition flux and, in the most elementary version of such a setup, basically directed perpendicular to the substrate. In vapor deposition experiments [4–6], the deposition flux possesses two characteristic properties: (i) It is typically low-energetic implying that no kick-off or even desorption of surface particles occurs and (ii) basically constant in space and time with some weak superimposed spatio-temporal fluctuations originating from the particle source. The particles from the beam are deposited at the surface and undergo various surface diffusion processes until they arrive at their final position. The growing layer build up by the deposited particles forms a spatio-temporally evolving free surface that is characterized by its *height* or *morphology* $H(\mathbf{x}, t)$ at time t and at the substrate location $\mathbf{x} = (x, y)$. Microscopically speaking, the evolution of the surface morphology results from the complicated and

only partly explored interaction of particles to be deposited at the surface and the already condensed particles. As experiments reveal [4–6], however, the evolution of the surface morphology on a mesoscopic scale is not just dominated by random spatial variations as in the case of random deposition. The observed type of pattern formation [4–6] suggests some type of, admittedly not perfect, underlying ordering phenomena that stem from the interplay of competing roughening and smoothing mechanisms.

Modern experimental investigation tools such as scanning tunneling microscopy combined with image processing allow for a detailed resolution of the surface morphology and its spatio-temporal evolution [4–6]. Since the obtained data set is too immense and the data also contain some degree of stochasticity due to the small deposition noise resulting from the particle source, the *height-height-correlation function*

$$C(r, t) = \langle \langle [H(\mathbf{x} + \mathbf{r}, t) - \langle H \rangle_{\mathbf{x}}][H(\mathbf{x}, t) - \langle H \rangle_{\mathbf{x}}] \rangle_{\eta} \rangle_{\mathbf{x}}, r = r \quad (1)$$

determines an appropriate quantitative statistical measure for the information on height variations and lateral correlations. In Eq.(1), $\langle \dots \rangle_{\eta}$ represents an average over different samples (ensemble average), $\langle \dots \rangle_{\mathbf{x}} = L^{-2} \int_0^L d^2 x \dots$ the spatial average over a sample area of size L^2 , and $\langle H \rangle_{\mathbf{x}} = \langle H \rangle_{\mathbf{x}}(t) = \langle H(\mathbf{x}, t) \rangle_{\mathbf{x}}$ the spatially averaged surface profile at time t . The height-height-correlation function $C(r, t)$ contains the two most important global quantities that characterize the surface morphology: (i) The *correlation length* $R_c(t)$ that is given by the first maximum of $C(r, t)$ for non-zero r , i.e. by $R_c(t) = \min\{r > 0 | \partial_r C(r, t) = 0, \partial_r^2 C(r, t) < 0\}$, and, therefore, determines the typical length scale over which height fluctuations are correlated, and (ii) the *surface roughness* $w(t)$ or root mean square deviation of the relative height fluctuations that is determined by the $r = 0$ -limit of $C(r, t)$, $w^2(t) = C(0, t)$. As a minimum requirement for a successful modeling attempt of the spatio-temporal evolution of $H(\mathbf{x}, t)$, the validation of the temporal evolution of $R_c(t)$ and $w(t)$ in comparison with the available experimental data needs to be achieved.

2 Model Equation for Amorphous Thin Film Growth

As a general tool for the understanding and interpretation of the growth dynamics, we use the concept of stochastic field equations [1–3]. This phenomenological approach disregards the microscopic details of the particle arrangement and interaction and considers the growth process on a slightly larger length scale, the nanoscale, where the (coarse-grained) surface morphology $H(\mathbf{x}, t)$ can be regarded as a field variable evolving continuously in space and time. Then, the first goal is to find an appropriate functional form for the spatio-temporal evolution equation of $H(\mathbf{x}, t)$ that is compatible with underlying physical symmetries of the growth process.

Assuming that the surface morphology $H(\mathbf{x}, t)$ is single-valued in \mathbf{x} or, physically speaking, that overhangs in the surface morphology do not appear, the general ansatz for the corresponding evolution equation reads [1–3]

$$\partial_t H = G[\nabla H] + I(\mathbf{x}, t) \quad (2)$$

where $I(\mathbf{x}, t)$ represents the deposition flux and the functional $G[\nabla H]$ comprises all physical mechanisms leading to growth and relaxational processes on the surface. In Eq.(2), the three most important symmetry requirements [2] for surface growth processes have been already incorporated: (i) no dependence of (2) on the specific choice of the origin of time (invariance under translation in time), (ii) no dependence of (2) on the specific choice of the origin of the coordinate system at the substrate (invariance under translation in the direction perpendicular to the growth direction), and (iii) no dependence of (2) on the specific choice of the origin of the H -axis (invariance under translation in growth direction). These symmetry requirements exclude any explicit dependence of the functional $G[.]$ on the time t , the spatial position \mathbf{x} , and the height H , respectively.

For vapor deposition experiments [4–6], the deposition flux is basically constant with some small superimposed stochasticity resulting from the particle source. As a consequence, the deposition flux can be split into a spatio-temporally constant mean deposition flux F and a fluctuating part $I(\mathbf{x}, t) = F + \eta(\mathbf{x}, t)$, where $\eta(\mathbf{x}, t)$ represents spatio-temporal Gaussian white noise given by $\langle \eta(\mathbf{x}, t) \rangle_\eta = 0$ and $\langle \eta(\mathbf{x}, t) \eta(\mathbf{x}', t') \rangle_\eta = 2D \delta(\mathbf{x} - \mathbf{x}') \delta(t - t')$. Here, $\langle \dots \rangle_\eta$ denotes the ensemble average, and D the fluctuation strength.

Since the mean deposition flux F is constant it also proves useful to introduce the height profile $h(\mathbf{x}, t) = H(\mathbf{x}, t) - Ft$ in the frame comoving with the velocity F . Then, (2) simplifies to

$$\partial_t h = G[\nabla h] + \eta(\mathbf{x}, t). \quad (3)$$

Specifically for amorphous growth processes, the isotropy of the amorphous phase implies *invariance under rotation and reflection* in the plane perpendicular to the growth direction. This excludes any odd derivatives of h in G and implies that ∇ -operators entering the various contributions in G must be multiplied in couples by scalar multiplication. Assuming that all surface relaxation processes are local, we finally expand the functional G in a power series in all possible spatial derivatives of h and keep only the terms that are linear or quadratic in h and only possess a maximum of four ∇ -operators. As a result of the afore-mentioned symmetries, the deterministic part of (3) can only consist of the terms $\nabla^2 h$, $(\nabla h)^2$, $\nabla^4 h$, $\nabla^2(\nabla h)^2$, $(\nabla^2 h)^2$, and $\nabla \cdot [(\nabla h)(\nabla^2 h)]$. The last term can be slightly rearranged in the form

$$\nabla \cdot [(\nabla h)(\nabla^2 h)] = \frac{1}{2} \nabla^2 (\nabla h)^2 + 2M \quad \text{with} \quad M = \det \begin{pmatrix} \partial_x^2 h & \partial_y \partial_x h \\ \partial_x \partial_y h & \partial_y^2 h \end{pmatrix}. \quad (4)$$

Consequently, a *systematic* expansion of the functional form of the growth equation (2) that takes into account (i) the specific symmetries of amorphous

film growth and (ii) all admissible combinations of terms being linear or quadratic in $h(\mathbf{x}, t)$ and containing up to a maximum of four ∇ -operators is given explicitly by [9]

$$\partial_t h = a_1 \nabla^2 h + a_2 \nabla^4 h + a_3 \nabla^2 (\nabla h)^2 + a_4 (\nabla h)^2 + a_5 (\nabla^2 h)^2 + a_6 M + \eta. \quad (5)$$

The rhs of Eq.(5) consists of two linear terms and four nonlinear terms in h . Eq.(5) contains several known limiting cases such as the Kardar-Parisi-Zhang (KPZ) equation, $\partial_t h = a_1 \nabla^2 h + a_4 (\nabla h)^2 + \eta$, being the paradigm for a stochastic roughening process [11] and the noisy Kuramoto-Sivashinsky equation [12], $\partial_t h = a_1 \nabla^2 h + a_2 \nabla^4 h + a_4 (\nabla h)^2 + \eta$.

So far, we have only determined the leading order functional form of the growth equation. This approach does not reveal any information on the sign of the coefficients a_i , $i = 1, \dots, 6$, and the physical significance of the corresponding terms in (5). Focussing on the physics of amorphous growth, the coefficients a_i will be connected to the underlying microscopic processes in the next section.

3 The Physics behind the Growth Equation

Guided by the principle that any mathematically admissible term might have some physical significance, we next relate all terms appearing in the growth equation (5) to the four competing microscopic mechanisms

- surface tension [13]
- concentration equilibration of deposited particles [14,15]
- steering of arriving particles [8]
- inhomogeneous density distribution [8,9]

that, as we shall see in the next section, seem to dominate physical vapor deposition and are all, at least at some stages of the growth process, important. Also the signs and the order of magnitude estimates of some coefficients in (5), as well as a physically motivated simplification of (5) are obtained.

The linear term proportional to a_2 in Eq.(5) can be interpreted as the result of a type of a microscopic surface tension effect as originally suggested by Mullins [13]. The basic idea behind this effect (cf. also the middle part of Fig. 2) is that the just deposited particles favorably move to positions at the surface that have positive curvature $\nabla^2 h > 0$ since there, the already condensed surface particles form a local vicinity with higher binding energy. This gives rise to a diffusion current $\mathbf{j}_m \propto \nabla(\nabla^2 h)$ that, depending on the local curvature, can be uphill or downhill. The divergence of this current, $-\nabla \cdot \mathbf{j}_m = a_2 \nabla^4 h$, contributes to the surface evolution in (5) with a_2 being necessarily negative. This term basically tries to minimize the area of the surface and, as a consequence, to smooth the surface morphology.

The nonlinear term proportional to a_3 can be related to the tendency of equilibrating the non-homogeneous concentration c of the deposited particles

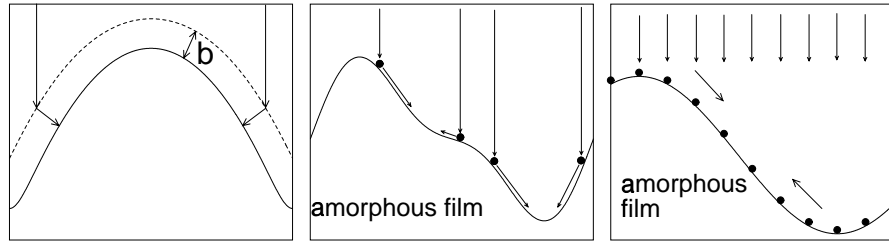


Fig. 2. Microscopic effects of amorphous surface growth. Left part: Inflection of particles due to interatomic interaction. Middle part: Surface diffusion of deposited particles due to surface relaxation. Right part: Equilibration of the inhomogeneous particle concentration due to the geometry of the surface

just after arriving at the surface. This effect has originally been suggested by Villain [14] (cf. also [15]). The underlying reason is of purely geometric nature. Although the deposition flux is basically homogeneous, more particles per surface area arrive at positions with a small or zero modulus of slope ∇h than at positions being strongly inclined with respect to the particle beam, cf. also the right part of Fig. 2. Therefore, the local concentration of the diffusing particles right after the deposition is not constant, but is weighted by the local slope of the surface, $c \propto 1/\sqrt{1 + (\nabla h)^2}$, or in a small gradient expansion, $c \propto 1 - \frac{1}{2}(\nabla h)^2$. Then, the tendency to equilibrate the concentration is reflected by a diffusion current $j_c \propto -\nabla c \propto \nabla(\nabla h)^2$, or, after taking the divergence, by the term $-\nabla \cdot j_c = a_3 \nabla^2(\nabla h)^2$ that contributes to the height changes in (5). Obviously, concentration equilibration requires that the coefficient a_3 is negative and also tries to smooth the surface morphology. A simple dimensional argument leads to an estimate for a_3 . Equation (5) implies that the coefficient a_3 has the dimension of $\text{length}^3/\text{time}$. The magnitude of a_3 necessarily depends on the deposition flux F that possesses the dimension of $\text{length}/\text{time}$ and the mean diffusion length l which is the only relevant length scale determining this process. The only combination of F and l leading to the correct dimension of a_3 is $F l^2$. Therefore, one expects $a_3 \propto -F l^2$. A thorough discussion of the concentration equilibration [8] supports this argument and yields the explicit relation $a_3 = -\frac{1}{8} F l^2$. Moreover, one expects that the typical magnitude of l is of the order of several atom diameters.

The two terms in (5) that are proportional to a_1 and a_6 can microscopically be related to the steering of the arriving particles. Here, the basic idea [8] is that the particles from the beam experience close to the growing surface a deflection due to the interatomic attractive interaction with the already condensed surface particles. As a consequence, the particles do not hit the surface perpendicular to the substrate orientation, but perpendicular to the surface itself. This implies that more particles arrive at positions at

the surface with negative curvature, $\nabla^2 h < 0$, than at positions with positive curvature $\nabla^2 h > 0$. Effectively, this leads to a tendency to roughen the surface morphology. We refer to Ref. [16] for experimental indications of the relevance of this effect. To model this scenario in a dynamical way [8], we use the idealization that the particles undergo a change of direction only after reaching a critical distance b , the effective range of the interaction, from the surface and are then attracted such that they arrive perpendicular to the surface, cf. the left part of Fig. 2. A detailed mathematical derivation [8] using a reparametrization in the coordinates of the imaginary surface where the interaction becomes effective (cf. the dotted line in the left part of Fig. 2) and a small gradient expansion in h in fact shows that this scenario gives simultaneously rise to the two contributions $a_1 \nabla^2 h$ and $a_6 M$ in (5). Moreover, the coefficients a_1 and a_6 can be related to the mean deposition flux F and the effective range b of the interatomic interaction yielding $a_1 = -Fb$ and $a_6 = Fb^2$ [8]. Although b cannot be directly measured its magnitude should be typically of the order of one atomic diameter and, therefore, much smaller than the radius of the surface curvature. This implies that the term proportional to a_6 is of minor relevance in comparison to the a_1 -term and can be neglected. Moreover, the sign of a_1 is negative.

The physical origin of the nonlinear terms proportional to a_4 and a_5 is determined by the potential variations of the coarse-grained density [7,8]. These terms cannot result from particle desorption since the substrate is held at room temperature and the particle energy in the vapor beam is rather low (typically of the order 0.1eV). Therefore, *all* arriving particles finally contribute to the surface growth. As a consequence, any term that cannot be recast in form of the divergence of a current in (5) arises from changes of the coarse-grained density. Assuming for the moment that the deposition noise is zero ($\eta = 0$), particle conservation implies that the rate of change of the number of particles per substrate area above a given substrate location, C , is determined by a balance equation $\partial_t C = -\nabla \cdot \mathbf{j}_C + \rho_0 F$. Here the divergence of the current \mathbf{j}_C is given by the combination of all surface relaxation processes (cf. the afore-mentioned arguments), i.e. by $-\nabla \cdot \mathbf{j}_C = \rho_0 [a_1 \nabla^2 H + a_2 \nabla^4 H + a_3 \nabla^2 (\nabla H)^2 + a_6 M]$. Allowing for density variations at the growing surface, the rate of change of C is related to the rate of change of the height H by $\partial_t C = \rho(\nabla H) \partial_t H$. Here $\rho(\nabla H)$ denotes the density at the surface. Without the incorporation of density changes ($\rho = \rho_0 = \text{const.}$), there is a direct proportionality $\partial_t C = \rho_0 \partial_t H$. If small density variations are taken into account, $\rho(\nabla H)$ can be expanded in the derivatives of H yielding $\rho(\nabla H) = \rho_0 [1 + q_1 (\nabla H)^2 + q_2 \nabla^2 H]$ in lowest order approximation. Therefore, $\partial_t H = \rho_0^{-1} [1 - q_1 (\nabla H)^2 - q_2 \nabla^2 H] \partial_t C$ holds. Inserting this in the balance equation from above, explains the presence of the two terms $-q_1 F (\nabla H)^2 = a_4 (\nabla h)^2$ and $-q_2 a_1 (\nabla^2 H)^2 = a_5 (\nabla^2 h)^2$ appearing in (5). From the physical point of view, however, density changes are primarily connected to the gradients of the surface profile reflecting the local arrangement

of the particles at the surface and not so much to the surface curvature. Therefore, it is pausable to disregard the term $a_5(\nabla^2 h)^2$ in a minimal description of the growth evolution. Since the density variations result from a widening of the mean inter-particle distances at the surface one has to expect that they locally decrease the density implying that $a_4 > 0$ holds.

Taking into account the afore-mentioned physical arguments, the terms $a_5(\nabla^2 h)^2$ and $a_6 M$ are negligible in leading order and, as a final result, we obtain the model equation for amorphous film growth [7–10],

$$\partial_t h = a_1 \nabla^2 h + a_2 \nabla^4 h + a_3 \nabla^2 (\nabla h)^2 + a_4 (\nabla h)^2 + \eta \quad (6)$$

with a_1, a_2, a_3 being negative and a_4 being positive.

Using stochastic numerical simulations of the surface growth equation (6) starting from a flat substrate (for details of the method see appendix C in [8]), we investigate in the remainder of this contribution the evolution of correlation length R_c and surface roughness w as a function of the experimentally measurable layer thickness \bar{H} . This quantity is determined by $\bar{H} = \langle \langle H(\mathbf{x}, t) \rangle_\eta \rangle_{\mathbf{x}} = Ft + \langle \langle h(\mathbf{x}, t) \rangle_\eta \rangle_{\mathbf{x}}$ and is, in general, implicitly connected to the time t via the solution of (6). The latter results from the fact that the surface profile generated by Eq.(6) possesses a finite excess velocity, $v = \langle \langle \partial_t h \rangle_\eta \rangle_{\mathbf{x}} = \langle \langle a_4 (\nabla h)^2 \rangle_\eta \rangle_{\mathbf{x}}$. Since a_4 is positive the average of the surface morphology $H(\mathbf{x}, t) = Ft + h(\mathbf{x}, t)$ grows with a faster speed than F as a result of the inhomogeneous density distribution.

4 Comparison with Experiments

In this section, we show that the model equation (6) is indeed able to quantitatively reproduce experimental data on the correlation length R_c and surface roughness w if the coefficients a_1, a_2, a_3, a_4 and D are appropriately chosen. For the specific example of the growth of $\text{Zr}_{65}\text{Al}_{17.5}\text{Cu}_{27.5}$ films [4–7], a parameter estimation procedure discussed in detail in [7] yields for the coefficients in (6) $a_1 = -0.0826\text{nm}^2/\text{s}$, $a_2 = -0.319\text{nm}^4/\text{s}$, $a_3 = -0.10\text{nm}^3/\text{s}$, and $a_4 = 0.055\text{nm}/\text{s}$ and for the strength of the deposition noise $D = 0.0174\text{nm}^4/\text{s}$. The experimentally determined mean deposition flux is given by $F = 0.79\text{nm}/\text{s}$. For this set of parameter values, we show the dependence of the correlation length R_c and surface roughness w (solid lines) on the thickness of the amorphous film in Fig. 3 and infer a very good agreement with the corresponding experimental data. For comparison, the corresponding results of the Kuramoto-Sivashinsky limit ($a_3=0$, dashed lines) are given. Since the correlation length ceases to exist at about 300nm in this limit we also conclude that both nonlinear terms proportional to a_3 and a_4 are necessary to reproduce the experimental data. Leaving off the term that describes the effect of density inhomogeneities, $a_4 = 0$, the surface roughness increases strongly with time and does not show the cross-over to a saturation at layer thicknesses of about 480nm (for more details of this limit cf. Ref.[8]). Moreover, both linear

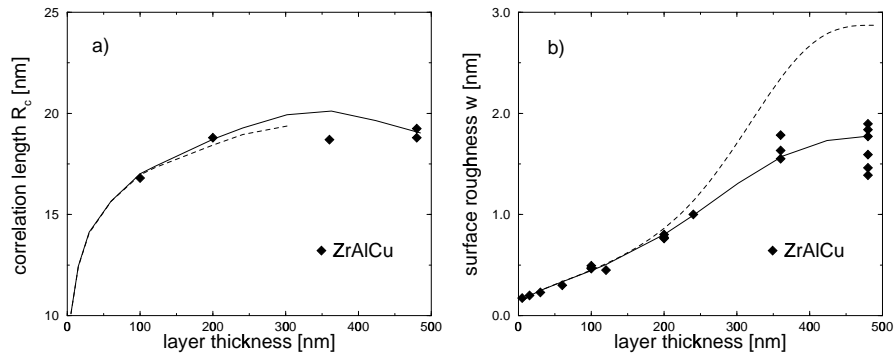


Fig. 3. Solid lines (dashed lines): Correlation length R_c and surface roughness w for the experimentally investigated thickness interval $0 \leq \bar{H} \leq 480\text{nm}$ calculated from the nonlinear growth equation (6) using the parameters $a_1 = -0.0826\text{nm}^2/\text{s}$, $a_2 = -0.319\text{nm}^4/\text{s}$, $a_4 = 0.055\text{nm}/\text{s}$, $D = 0.0174\text{nm}^4/\text{s}$ and $a_3 = -0.10\text{nm}^3/\text{s}$ ($a_3 = 0\text{nm}^3/\text{s}$). Diamonds represent the corresponding experimental results. This figure is taken from Ref.[7]

terms proportional to a_1 and a_2 are necessary to excite the growth instability at the initial stages of the growth process [8]. Consequently, Eq.(6) must be considered as a minimal model for the growth of amorphous $\text{Zr}_{65}\text{Al}_{17.5}\text{Cu}_{27.5}$ films.

The extrapolated parameters a_1 , a_2 , a_3 , a_4 , and D also allow for microscopic estimates [7]. (i) Since $a_1 = -Fb$, the typical range b of the interaction between the surface atoms and the particles to be deposited is about 0.1nm , i.e. of the size of the radii (0.2nm) of the surface atoms. (ii) Since $a_3 = -Fl^2/8$, the diffusion length l is about 1.0nm . Consequently, the deposited particles experience a surface diffusion on a nanometer scale and do not just stick at the places where they hit the surface. (iii) If the particles arrive independently on the surface, the deposition noise is related to the particle volume Ω and the mean deposition rate F by $2D = F\Omega$ [8], yielding $\Omega = 0.04\text{nm}^3$. This is up to a factor of two the averaged particle volume of ZrAlCu . (iv) The local density of the growing film varies with the surface slope: On an inclined surface area the local density is decreased by $\rho(\nabla h) = \rho_0/\gamma$ with $\gamma = 1 + (a_4/F)(\nabla h)^2$ (where a_4/F is about 0.07). These finite density variations are physically compatible with the small diffusion length l of two to three atom diameters. At the layer thickness 480nm , this local density reduction γ (averaged over the surface) possesses a mean 1.021 and a standard deviation 0.017 .

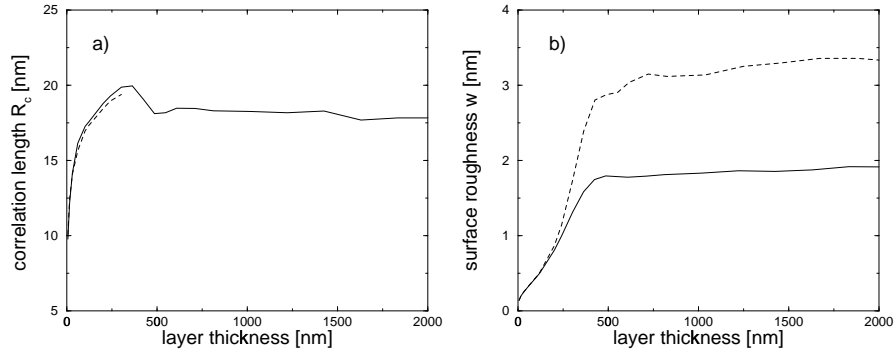


Fig. 4. Solid lines (dashed lines): Correlation length R_c and surface roughness w for the thickness interval $0 \leq \overline{H} \leq 2000\text{nm}$ calculated from the nonlinear growth equation (6) using the parameters $a_1 = -0.0826\text{nm}^2/\text{s}$, $a_2 = -0.319\text{nm}^4/\text{s}$, $a_4 = 0.055\text{nm}/\text{s}$, $D = 0.0174\text{nm}^4/\text{s}$ and $a_3 = -0.10\text{nm}^3/\text{s}$ ($a_3 = 0\text{nm}^3/\text{s}$)

5 Some Predictions based on the Growth Equation

In this section, we explore some further properties of the growth process in a layer thickness range up to 2000nm that has so far not yet experimentally investigated. The results in Fig. 3 up to a layer thickness of 480nm suggest that the growth process has not yet reached a final, not necessarily stationary state. Using again the afore-mentioned parameter values, the dependence of the correlation length R_c and surface roughness w (solid lines) on the thickness of the amorphous film is shown in Fig. 3 (the dashed lines refer to the special case $a_3=0$). Obviously, the surface roughness has reached an almost constant value for a layer thickness larger than 600nm that increases only very weakly as the growth process proceeds. In contrast to that, the correlation length steeply decays after reaching a maximum and then saturates in an almost constant value for a layer thickness larger than 600nm as the growth process proceeds. For further results, in particular the properties of the correlation function and the related height difference correlation function as well as visualizations of the surface morphology and a theoretical interpretation of the various stages of the growth process, we refer to Ref.[10].

To obtain further insight into the spatio-temporal evolution of the surface morphology, we present in Fig. 5 a representative one-dimensional cross-section of the growth of the surface profile (for $y = 0$) with increasing time or layer thickness. For demonstration purposes, the relative height fluctuations have been weighted by a factor of 20 relative to the mean thickness $\langle H \rangle_{\mathbf{x}} = \langle H \rangle_{(x,y)}$. From Fig. 5, three remarkable features can be read off. First, as the time proceeds and the layer builds up, the surface morphology develops into a predominantly almost periodic structure with an averaged periodicity length given by the correlation length R_c and some superimposed stochastic

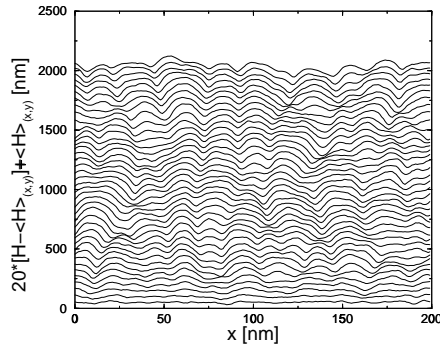


Fig. 5. Visualization of the cross-section of the spatio-temporal evolution of the growing surface of the film

variations. Second, the evolving mound and dip structure is asymmetric in the sense that the dips are comparatively narrow in contrast to the wide mounds. Third and most remarkably, the surface morphology does not approach a stationary profile in the thickness range $1000\text{nm} \leq \langle H \rangle_{(x,y)} \leq 2000\text{nm}$. Despite the fact that statistical quantities such as the correlation length and the surface roughness are almost constant in this thickness interval, the surface profile still varies significantly with time.

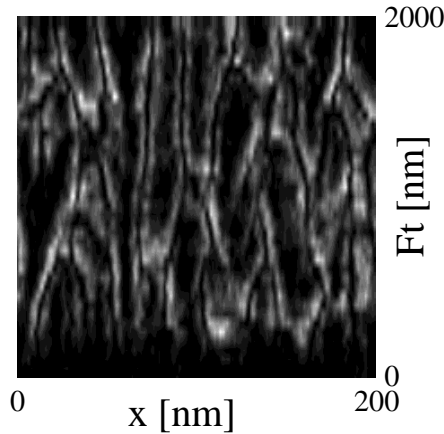


Fig. 6. Visualization of the spatial density variations in a cross-section of the bulk of an amorphous film of the height $Ft = 2000\text{nm}$ using numerical simulations of Eq.(6). For further details cf. main text

As we have argued in section 3 and 4, density inhomogeneities on nano-scales seem to play a non-negligible role for the understanding of amorphous film growth. Consequently, one has to expect that the whole grown film also exhibits some, albeit small spatial density variations provided that the density inhomogeneities of the material at the surface are frozen as the growth process advances. To demonstrate this effect, we present in Fig. 6 a visualization of a numerical calculation of the density distribution in a representative cross-section ($y = 0$) of a film grown up to a height of $Ft = 2000\text{nm}$. To this

end, we have calculated the local density reduction $\gamma - 1 = \rho_0/\rho(\nabla h) - 1 = (a_4/F)(\nabla h)^2$ using the afore-mentioned parameter values for $Zr_{65}Al_{7.5}Cu_{27.5}$ and ∇h from a corresponding simulation of Eq.(6). Note that the local density reduction vanishes at the maxima and minima of the surface profile, $\gamma = 1$ (marked in black in Fig. 6), whereas γ reaches its maximum values at places of the steepest inclination of the surface profile (marked in white in Fig. 6) implying a smaller local density. Between these extrema, there is a gradual change of the local density (marked by the different grey scales). Therefore, the wide dark vertical stripes are the relics of the mounds of the growing surface profile, whereas the small dark vertical stripes are the relics of the corresponding narrow valleys. The relative density difference between the black and white areas is typically about ten percent.

6 Conclusion

As the major point of our contribution, we have demonstrated that the concept of stochastic field equations applied to the surface morphology of growing amorphous films (i) provides valuable insights in underlying microscopic surface relaxation mechanisms of the growth process and (ii) even leads to a *quantitative* agreement of characteristic measures of the spatio-temporal surface morphology with experimental data.

Acknowledgement: This work has been supported by Sonderforschungsbereich 438 (TU München/Univ. Augsburg), Project A1. We thank M. Moske, K. Samwer, S. G. Mayr, and D. E. Wolf for useful conversations.

References

1. W. M. Tong, R. S. Williams: *Annu. Rev. Phys. Chem.* **45**, 401 (1994)
2. A.-L. Barabasi, H. E. Stanley: *Fractal concepts in surface growth* (Cambridge Univ. Press, Cambridge, 1995)
3. M. Marsili, A. Maritan, F. Toigo, J. Banavar: *Rev. Mod. Phys.* **68**, 963 (1996)
4. B. Reinker, M. Moske, K. Samwer: *Phys. Rev.* **B 56**, 9887 (1997)
5. S. G. Mayr, M. Moske, K. Samwer: *Europhys. Lett.* **44**, 465 (1998)
6. S. G. Mayr, M. Moske, K. Samwer: *Phys. Rev.* **B 60**, 16950 (1999)
7. M. Raible, S. G. Mayr, S. J. Linz, M. Moske, P. Hänggi, K. Samwer: *Europhys. Lett.* **50**, 61 (2000)
8. M. Raible, S. J. Linz, P. Hänggi: *Phys. Rev. E* **62**, 1691 (2000)
9. S. J. Linz, M. Raible, P. Hänggi: *Lect. Notes Phys.* **557**, 473 (2000)
10. M. Raible, S. J. Linz, P. Hänggi: *Amorphous thin film growth: effects of density inhomogeneities*, submitted for publication
11. M. Kardar, G. Parisi, Y. C. Zhang: *Phys. Rev. Lett.* **56**, 889 (1986)
12. J. T. Drotar, Y.-P. Zhao, T.-M. Lu, G.-C. Wang: *Phys. Rev. E* **59**, 177 (1999)
13. W. W. Mullins: *J. Appl. Phys.* **28**, 333 (1957); *J. Appl. Phys.* **30**, 77 (1959)
14. J. Villain: *J. Physique I* **1**, 19 (1991)
15. M. Moske: *Mechanische Spannungen als Sonde für Schichtwachstum und Schichtreaktionen* (Habilitation thesis, Universität Augsburg, 1997)
16. S. van Dijken, L. C. Jorritsma, B. Poelsema: *Phys. Rev. Lett.* **82**, 4038 (1999)